

1 Groundwater vulnerability to pollution in karst aquifers, considering key challenges and
2 considerations: application to the Ubrique springs in southern Spain
3

4 Ana I. Marín ^{(1)*}, José Francisco Martín Rodríguez ⁽²⁾, Juan Antonio Barberá ⁽²⁾, Jaime Fernández-Ortega ⁽²⁾, Matías
5 Mudarra ⁽²⁾, Damián Sánchez ⁽²⁾ and Bartolomé Andreo ⁽²⁾

6 (1) European Topic Centre of University of Malaga (ETC-UMA), 29071 Málaga, Spain

7 (2) Department of Geology and Centre of Hydrogeology, University of Málaga (CEHIUMA), 29071 Málaga, Spain

8 * Corresponding author: aimarin@uma.es. ORCID: 0000-0002-8519-3918
9

10 **Abstract**

11 Groundwater vulnerability mapping is one of the tools most often applied to analyse the
12 sensitivity of karst aquifers to pollution. These maps aim to support stakeholders in decision-
13 making and to promote land-use management compatible with water protection. However, the
14 validation of these maps is still a challenge in many cases, triggering high uncertainty. For karst
15 media, due to the strong heterogeneity in recharge mechanisms and hydraulic characteristics,
16 validation is a significant stage and it must be inherent within the groundwater vulnerability
17 assessment process. This work aims to assess the implementation of tools used for protecting the
18 quality of water discharging or extracted from the Ubrique karst system in southern Spain, which
19 supplies drinking water that is threatened by periodical pollution/turbidity episodes. A
20 groundwater vulnerability map, attained by application of the COP method and validated by
21 multiple in-situ observations, shows an extremely vulnerable system due to the absence of
22 protective overlayers and the significant development of exokarst landforms, including shallow
23 holes. This map could constitute the basis for defining protection zones for the Ubrique springs.
24 However, their comprehensive protection requires the implementation of monitoring tools and an
25 effective management strategy, through an early warning system that assures stable

26 environmental and hydrogeological conditions and improves operational procedures associated
27 with the drinking water service. This research establishes the strong relationship of the different
28 methods applied to protect the source from contamination events, ranging from classical
29 hydrodynamic and hydrochemical approaches to the implementation of protection zones and
30 early warning groundwater quality monitoring networks.

31

32 **Keywords:** Karst, Vulnerability mapping, Groundwater protection, Early warning system, Spain.

33

34 **NOTE TO COPYEDITOR – PLEASE INSERT THE FOLLOWING AS A FIRST-PAGE FOOTNOTE:**

35 Published in the special issue “Five decades of advances in karst hydrogeology”

36

37

38

39 **1 Introduction**

40 The concept of the “contamination vulnerability” of an aquifer has been defined by many authors (Margat 1968; Foster
41 1987; Zaporozec 1994; among others) as the sensitivity to contamination of the groundwater resource, taking into
42 account the geological, hydrologic and hydrogeological characteristics of the aquifer, independently from the nature
43 and scenario of the contamination (Daly et al. 2002; Zwahlen 2004). This is the adopted definition for “intrinsic
44 vulnerability”, but if the pollutant properties are considered during the vulnerability evaluation, then it is redefined as
45 the “specific vulnerability”. Although the nature of the pollutant influences the contamination pattern throughout the
46 aquifer, in most cases vulnerability mapping is based on the intrinsic concept, in order to simplify the vulnerability
47 schemes and its transference as a tool for water protection and land-use planning. The principal objective of
48 contamination vulnerability mapping is to identify and highlight the most vulnerable zones within catchment areas, as
49 well as to provide unified criteria for protecting the groundwater resources. Vulnerability to pollution is not a
50 characteristic that can be directly measured in the field, so indirect methodologies for vulnerability assessment are

51 required. In fact, the degree of groundwater vulnerability to pollution does not remain stable along time but varies
52 according to the specific characteristics of each case.

53 The importance of karst aquifers as sources of good quality drinking water is well accepted worldwide. Roughly 20–
54 25% of the world's population depends on water supplies from karst aquifers, directly or indirectly, and 10-15% of
55 the world's land surface area has karst aquifers beneath it (Ford and Williams, 2007; Goldscheider et al. 2020). Karst
56 groundwater is particularly sensitive to contamination, due to aquifer inner structure and hydrogeological behavior,
57 which determine the rapid transfer of recharge waters and their fast distribution over large distances, achieving high
58 flow velocities and short residence time. Consequently, the self-cleaning capacity of the karst groundwater is
59 commonly low or very low (Doerfliger and Zwahlen 1998; Ford and Williams 2007). Therefore, karst aquifers require
60 specific methodologies for vulnerability mapping which take into account their specific intrinsic properties (Zwahlen
61 2004).

62 A set of combined approaches, specifically adopted for karst environments, has been developed on the basis of the
63 guidelines of the European COST Action 620, including –among others- the PI method (Goldscheider et al. 2000),
64 the COP method (Vías et al. 2006), the Slovene Approach (Ravbar and Goldscheider 2007), and the PaPRIKa method
65 (Kavouri et al. 2011). Spatial information and geographic information system (GIS)-based approaches are widely used
66 for intrinsic vulnerability mapping of karst aquifers, although there are also relevant advances in geological and
67 hydrogeological modeling (Butscher and Huggenberger 2008; Jeannin et al. 2013; Hartmann et al. 2013; Turk et al.
68 2014; Ghasemizadeh, et al. 2016).

69 In practice, the assessment of the aquifer vulnerability to pollution (at whatever scale) inevitably involves
70 simplification of the naturally complex geological framework and related hydrological processes. Although this is a
71 powerful tool, it incorporates a significant but variable level of uncertainty during mapping development and is not
72 readily capable of independent calibration (Foster et al. 2013). In addition, the application of different methods on the
73 same test site, using the same database, often leads to significant differences in mapping results (Vías et al. 2005;
74 Neukum and Hötzl 2007; Ravbar and Goldscheider 2009; Marín et al. 2012). For these reasons, the validation of the
75 vulnerability maps is a key element that has to be implemented as part of the vulnerability assessment, within a holistic
76 perspective. Validation may involve a wide range of methods and techniques such as field tracing experiments,
77 analysis of natural responses of karst springs, study of environmental tracers, numerical modelling, etc. (Marín et al.

78 2015). Despite the importance of mapping validation in the context of groundwater protection and management, this
79 phase is still bypassed in many cases. However, since the final goal of the entire methodological process is to
80 implement strategies for groundwater protection (i.e. protective zoning around abstraction points), as part of effective
81 land-use planning, this needs to be inherent to the vulnerability assessment process in karst.

82 This paper aims to present the main advances related to vulnerability assessment of karst groundwater resources to
83 pollution, highlighting the present challenges and new directions to perform this type of mapping under the complex
84 scenario of karst aquifers. The test site, Ubrique aquifer (Cádiz province, southern Spain), needs a dynamic protection
85 and management plan of karst groundwater resources due to the impact of high-turbidity peaks and associated bacterial
86 contamination episodes threatening the drinking water supply. In Spain, the applied water legislation, i.e. the Royal
87 Decree 140/2003 of 7 February, establishes the sanitary criteria and chemical thresholds for the quality of potable
88 water for human consumption among which are the mentioned parameters that generate operational constraints in
89 Ubrique drinking water supply. Consequently, this test site gathers conditions to implement an effective decision-
90 support system (DSS) in order to improve operational procedures in drinking water services.

91 All the stages that should be conducted during the adoption of an effective system for protecting groundwater against
92 contamination are illustrated in the present work. The procedure, which is not unidirectional, but rather feeds back
93 from the interactions of the different stages, consists of: (1) hydrogeological characterization of the test site, gathering
94 information on significant karst features; (2) implementation of a suitable holistic approach as a methodology for
95 vulnerability mapping; (3) the validation method, with a particular focus on data requirements to implement this stage;
96 (4) discussion of the potential role and applicability of the adopted methodology according to the understanding of the
97 hydrogeological background and validation results; and finally (5) testing the implementation of the common and
98 newly developed approaches for safeguarding groundwater resources by means of early warning systems (EWS).

99

100

101 **2 Test site**

102 The study area is the Ubrique karst aquifer, a hydrogeological system of area 26 km² located within a larger
103 mountainous region known as Sierra de Grazalema, in Cadiz province, southern Spain (Fig. 1). The mountainous relief
104 ranges from 400 to 1,500 m above sea level (a.s.l.), being the highest elevations associated with the NE-SW

105 alignments. The climate is humid Mediterranean, with a marked seasonal pattern in the annual variations of
106 precipitation and air temperature. Rainfall occurs from autumn to spring times, associated with wet winds coming
107 from the Atlantic Ocean. Climate conditions are also characterized by a dry season (very often of up to 3–4 months),
108 practically without rain, in summer. The mean annual precipitation in this area, calculated from isohyets maps, was
109 around 1,350 mm for the period of hydrological years 1965 - 2006, with a spatial distribution influenced by the
110 elevation: it was below 1,000 mm in the lower parts (southwestern border) and up to 1,600 mm in the higher areas
111 (Andreo et al. 2014). The air temperature records show mean annual values from 14 to 16 °C, depending on the
112 elevation.

113 From a geological standpoint, the experimental field site and the other reliefs that make up the Sierra de Grazalema
114 area are situated within the Betic Cordillera; this consists of (from the bottom to the top): Upper Triassic (Keuper)
115 clays, dolomitic beds, sandstones and evaporite rocks (mainly gypsum), Jurassic dolostones (lower) and limestones
116 (upper) -500 m thick-, and Cretaceous-Paleogene marly-limestones and marls (Martín-Algarra 1987). The geological
117 structure is characterized by open anticline folds whose axes plunge towards the SW and tight synclines matching
118 with depressions constituted by younger marly-limestones materials. Over the previous rocks and overthrusting them
119 appear outcrops of Tertiary flysch-type clays and sandstones. The entire structure is affected by more recent strike-
120 slip faults (NW-SE) and normal fractures (NNW-SSW and N-S) which configure the geological structure and
121 orography of the area. The predominance of Jurassic oolitic limestones, densely fractured, jointly with bedding planes
122 and the prevailing climate conditions, reinforce karstification phenomena and a noteworthy development of exokarst
123 landforms over the bare carbonate outcrops. These include large karrenfields, dolines, uvalas and swallow holes
124 (Delannoy 1987). The presence of low-permeability rocks (marls and clays) in syncline cores, sometimes affected by
125 inverse faults, result in the establishment of endorreic areas, whose natural drainage occurs through swallow holes
126 (Figs 1 and 2) hydrologically connected with shafts and other endokarst features.

127 In hydrogeological terms, the Ubrique aquifer is formed by fractured and karstified Jurassic carbonate rocks, limited
128 by low-permeability materials at all their borders (flysch clays, Cretaceous-Tertiary marls, and Triassic clays). The
129 exception is a 1-km-long open limit on the northeast edge, delineated after the interpretation of the results derived
130 from the multitracer tests considered in the present work. The geometry of the aquifer is particularly determined by
131 the anticlinorium folds that define respectively the Sierra de Ubrique and the Sierra del Caillo, and locally by a NE-
132 SW inverse fault affecting the syncline structure located between previous ones. The Ubrique aquifer is a binary karst

133 system with the interpretation expressed by Bakalowicz (2005) and Mayaud et al. (2014) among others, since duality
134 in recharge mechanisms was proved: more or less diffuse infiltration from rainfall through the carbonate outcrops
135 (autogenic component), and the concentrated infiltration of water runoff from a small neighbour catchment formed by
136 low-permeability materials (flysch clays and Cretaceous marls; Fig 1). Superficial allogenic input enters the system
137 through the Villaluenga del Rosario shaft. This represents one of the most important hotspot in the aquifer from the
138 protection of groundwater perspective. On the other hand, natural drainage occurs through the permanent and temporal
139 (overflow) springs located at the SW border of the aquifer. The most significant ones are the Cornicabra (located at
140 349 m a.s.l.) and Algarrobal (317 m a.s.l.) perennial outlets, which have discharge rates of 10 to 2,460 l/s (mean 406
141 l/s) and 10 to 2,625 l/s (mean 157 l/s), respectively. Additionally, several overflow springs appear in this sector at
142 increasingly higher elevations during high flow; the most relevant is Garciago spring (422 m a.s.l.) whose discharge
143 rate is, on average, 311 l/s but ranges from 0 to 6,059 l/s (Sánchez et al. 2018). Cornicabra and Algarrobal supply
144 drinking water for the neighbour village, Ubrique (18,000 inhabitants). These springs are periodically affected by high
145 turbidity peaks linked to inorganic sediment particles during stormy periods but also to the runoff water infiltrated in
146 the Villaluenga del Rosario shaft, that lixiviates the fecal remains of the livestock from the endorreic area and receives
147 partially treated waste water from 500 inhabitants. These turbidity episodes generate operational constraints and hinder
148 the exploitation of the available water resources from the aquifer.

149 Since the test site is a part of Sierra Grazalema Natural Park, and as a result of its valuable environmental, botanical
150 and faunistic aspects, the conservation of natural conditions has been a priority for the different administrations.
151 Consequently, livestock farming (primarily cattle), leather production and active tourism represent the only significant
152 economic activities in this protected area. Vegetation is mostly Mediterranean shrub and pasture, except for the highest
153 areas, where there is neither soil development nor vegetation. Two main soil types can be distinguished: the carbonate
154 outcrops are covered by patchy leptosols and regosols, whereas less permeable soils with a thickness of 10–70 cm and
155 a silty–clayey texture overlie Cretaceous marl outcrops.

156

157 **3 Methodology**

158 3.1 Hydrogeological characterization

159 The implementation of one of the already existing methods for vulnerability mapping presents, *a priori*, two key
160 issues: a comprehensive understanding of the hydrogeological characteristics and behavior of the site where the
161 methodology will be implemented, and sufficient technical knowledge of the GIS tools used. Regarding the GIS skills,
162 in many cases, this is easily afforded by means of training and tutorials, being directly replicable for all the aquifers
163 assessed. Nevertheless, the most crucial element in vulnerability mapping in karst is the consistent hydrogeological
164 knowledge applied as expertise. Since karst aquifers are individually different in terms of distinctive behavior and
165 characteristics (geological, climatological, hydrological, land uses, etc.), specific site knowledge is necessary.

166 The hydrogeological characterization encompasses jointly qualitative and quantitative analyses of the information
167 derived from geological, geophysical and speleological methods, hydrological and hydraulic techniques, and the use
168 of natural tracers, such as isotopes and hydrochemical parameters, as well as the application of dye tracer tests
169 (Goldscheider and Drew 2007; Hartmann et al. 2014; Stevanovic 2015; Mudarra et al. 2019). This allows the
170 implementation of the vulnerability mapping methodology and its later validation, enhancing the reliability and
171 accuracy of the results from the mapping procedure.

172 The type of recharge (concentrated or diffuse *versus* allogenic or autogenic), the flow conditions within the system
173 (conduit or diffuse flow) and the storage capacity of the aquifer are the major factors controlling the functioning of
174 the aquifer (Goldscheider and Drew 2007). Since vulnerability mapping involves a spatially explicit model, the most
175 basic information includes a definition of the limits and geometry of the aquifer and the consequent dimensions of its
176 catchment area, which are used as a reference to implement the methodology. The vulnerability map must cover the
177 recharge area extent, including the allogenic area if this contributes significantly to the aquifer recharge or spring
178 behaviour. In this way, the analysis of natural and artificial (dye) tracer records has been increasingly used in karst
179 hydrogeology to identify the flow paths, to delineate recharge areas, and to characterize solute transport processes
180 (Batiot et al. 2003; Celle-Jeanton et al. 2001; Andreo et al. 2006; Perrin et al. 2007; Goldscheider et al. 2008; Barberá
181 et al. 2018; among others).

182 In addition, the analysis of spatial variations of groundwater chemistry within aquifers, but also temporal evolution of
183 selected hydrochemical parameters (chemographs), help to understand the groundwater's hydrogeological behavior,
184 providing realistic information under different hydrological conditions (flood, recession, depletion, etc.). Some of the

185 characteristics that define the hydrogeological functioning of a karst system, such as the degree of functional
186 karstification (the active karst network that permits the flow path integration through the aquifer from the surface to
187 the spring, Mudarra and Andreo 2011) or water sources and mixing, can be inferred from the joint analysis of chemical
188 constituents integrating chemographs, including natural tracers of infiltration (such as intrinsic fluorescence), total
189 organic carbon (TOC), and NO_3^- (Hunkeler and Mudry 2007; Mudarra et al. 2014; Barberá and Andreo 2012). These
190 parameters must be clearly characterized and properly assessed in order to define correct protection strategies for the
191 karst groundwater.

192 Detailed hydrogeological investigations, including dye tracer tests, have been carried out in the Ubrique aquifer since
193 2012 (Sánchez et al. 2016; Martín-Rodríguez et al. 2016; Sánchez et al. 2017). These original investigations enabled
194 researchers to define the recharge area, to perform water budget computations, to infer the hydrological and
195 hydrodynamic behaviour, and to document most of the environmental characteristics of the test site, i.e. climate, soil
196 mapping, flow concentration within the epikarst, etc. Although most of the methods for groundwater vulnerability
197 mapping aims to be applied using geo-environmental data available in most countries, some fieldworks for adjusting
198 or tailoring the previous geodatabase to fit the vulnerability topic were done within the context of these research
199 projects (see section '*Results and discussion*').

200

201 **3.2 Groundwater vulnerability mapping**

202 The objective of contamination vulnerability mapping is to identify the most vulnerable zones within catchment areas,
203 providing scientific reliable criteria for groundwater protection. The vulnerability to pollution of an aquifer is not
204 directly measurable in the field, so indirect methods for its assesment are required. These widely used approaches
205 are based on multiparametric analyses (on overlay and index techniques), with the assistance of GIS-based tools, relying
206 on the quantitative or semiquantitative compilation and interpretation of mapped data (Gogu and Dassargues 2000). GIS
207 allows for matching data on the characteristics of the study aquifer keeping the geographical framework as reference.
208 Each parameter represents the variables involved in groundwater vulnerability that are discretized using scored
209 intervals according to the relative degree of sensitivity to contamination.

210 As mentioned above, karst aquifers are particularly vulnerable to contamination due to flow concentration within the
211 epikarst layer and concentrated recharge via swallow holes. As a result, contaminants may easily reach the saturated

212 zone and then be rapidly transported through karst conduits over large distances (Goldscheider 2005). Many methods
213 have been developed to assess groundwater vulnerability to contamination. These include methods that take account of the
214 geological, hydrological, and hydrogeological characteristics of a karst system and climate variables, such as precipitation
215 dynamics. Two types of vulnerability assessment can be differentiated (Daly et al. 2002): for the resource and for the source.
216 According to the European guideline for vulnerability mapping (Zwahlen 2004), the assessment of resource vulnerability
217 considers processes that control the flow of infiltrated water from the surface (all the modalities) to the main phreatic zone.
218 An additional characterisation of groundwater flow through the saturated zone makes possible the mapping of the
219 vulnerability of a water source.

220 In this work, the COP method has been selected for mapping the groundwater vulnerability of the experimental area.
221 This method was primarily designed for resource vulnerability assessment (Vías et al. 2006), being later adapted for
222 source vulnerability assessment, namely COP+K (Andreo et al. 2009). The COP method, worldwide applied (Vías et
223 al. 2006; 2010; Yildirim and Topkaya 2007; Polemio et al. 2009; Katsanou and Lambrakis 2017; among other), has
224 been successfully implemented in karst areas with similar climate and geological frameworks to Ubrique aquifer (Marín
225 et al. 2012).

226 The COP method uses variables, parameters and factors in agreement with those proposed in the European Approach.
227 Then, relevant factors deal with the permeability and thickness of the soil and rock composing the unsaturated zone
228 (named O factor) and the concentration of runoff as influenced by topography, the karst features and the vegetation
229 cover (C factor), and the distribution and intensity of precipitation (P factor). The COP vulnerability index value is
230 obtained by multiplying the C, O and P scores.

231 The addition of the K factor, which considers the characteristics of water flow in the saturated zone, allow for mapping
232 the source vulnerability. This map helps to define or redefine the protection zones of the karst aquifers that should
233 support the decision makers when considering water supply protection and should promote sustainable development
234 of the aquifer and surroundings (Marin et al. 2015).

235

236 **3.3 Statistical assessment**

237 The statistical assessment of the results derived from vulnerability tasks was done by the application of ordinary least
238 squares (OLS) regression. Using the OLS tool-box (Arc-GIS® 10.7 ESRI Inc.), it is possible to evaluate relationships

239 between the explanatory variables (input variables used for vulnerability mapping by COP) and the dependent variable
240 (COP value). The tool provides statistical information for each explanatory variable in the model, about the coefficient
241 and the robust probability. The “coefficient” (hereafter as Coef.) represents the strength and type of relationship
242 between each explanatory variable and the dependent variable while the “probability” (Prob.) determines the
243 coefficient significance, based on the T test. In addition, the scatterplot depicts the relationship between an explanatory
244 variable and the dependent variable. Strong relationships appear as diagonals and the direction of the slope indicates
245 if the relationship is positive or negative.

246 Dependent and explanatory variables should have numerical fields containing a variety of values. For the application
247 of the OLS tool, in addition, the variables must be discretized. The vulnerability map, which was produced in raster
248 format at pixel size 5 x 5 m, has been resampled to 50 x 50 m, generating a database of 11,060 points within the
249 Ubrique aquifer extent.

250 The input variables of COP were screened to select those that accomplish with the requirements: soil subfactor (OS,
251 meaning soil characteristics), lithology subfactor (OL, related to the attenuation capacity of each layer within the
252 unsaturated zone), lithology degree of fracturing (ly), thickness of unaturated zone (zns), slope and vegetation
253 characteristics (sv), surface karstic features, that include the distances to swallow hole within the scenario 1 (Karst_f),
254 mean annual rainfall of a historical series of wet years (Pq) and intensity of precipitation (P_int).

255

256 **3.4 Validation**

257 Vulnerability maps can be validated by means of several methods (Zwahlen 2004), such as analysis of the
258 hydrochemical responses of the karst springs, solute transport dynamics (natural or artificial) and/or by the use of
259 hydrodynamic modeling approaches. Each of these procedures informs us about the single or a limited number of
260 hydrological processes within the aquifer. To obtain a comprehensive understanding that leads to an accurate
261 validation, it would be necessary to use a wide range of approaches to characterize both fast and slow flows within
262 the system, recharge mechanisms, aquifer responses in both high and low water conditions, system dynamics at event-
263 scale and, in general, the aquifer functioning. The hydrodynamic response of the spring water, especially during
264 recharge periods, in conjunction with hydrogeochemical properties, has been largely used in a complementary way to
265 characterize the hydrogeological functioning of karst aquifers (Shuster and White 1971; Mudry 1987; Genthon et al.

266 2005). In addition to the hydrodynamics, which constitutes the most elementary tool for validation, the temporal
267 evolution of natural tracers of rapid infiltration (originating in the soil layer), and dye tracer tests specifically adapted
268 to check the vulnerability to pollution, are the most powerful set of tools to validate the vulnerability maps in karst
269 regions (Perrin et al. 2004; Marin et al. 2015). Yet because natural and dye tracers complement each other, their joint
270 use can enhance our understanding of karst aquifer processes (infiltration, recharge and vulnerability), as noted by
271 Marín and Andreo (2015).

272 In this work, the validation of the vulnerability map has been done using the time series of TOC and NO_3^- contents
273 and turbidity values detected in the spring waters, coupled to hydrodynamic responses. In addition, the results of two
274 previous tracer tests carried out in the framework of hydrogeological investigations have been used to characterize the
275 concentrated recharge and to calculate flow velocities for inferring vulnerability classes.

276

277 **4 Results and discussion**

278 **4.1 Hydrogeological characterization for implementing vulnerability mapping**

279 Ubrique aquifer shows favorable features for vulnerability mapping applications given its confirmed duality in
280 recharge mechanisms but also a well-defined geometry inferred by hydrogeological criteria, after several years of
281 investigations (Sánchez et al. 2016; Martín-Rodríguez et al. 2016; Sánchez et al. 2017). The recharge area of the
282 aquifer is well defined by tracer tests and water balance assessment (Fig. 1). According to the hydrodynamic
283 information, the total discharge measured from all springs draining the Ubrique aquifer accounted for $35.1 \text{ hm}^3/\text{year}$
284 during the period 2012 - 2015 (Martín-Rodríguez et al. 2016). On the other hand, mean annual values of diffuse
285 recharge were indirectly assessed using the soil water balance method, after application of the Hargreaves and Samani
286 (1985) approach for evaluation of the potential evapotranspiration (50 mm of useful reserve in the soil according to
287 the edaphic properties of the experimental area). From these values, an effective rainfall value of $31.4 \text{ hm}^3/\text{year}$ was
288 calculated for the study area, equivalent to the diffuse recharge occurring over 26 km^2 of carbonate outcrops. In
289 agreement with these results, the average total outputs exceed the input value by $3.7 \text{ hm}^3/\text{year}$. The difference mainly
290 corresponds to the relative allogenic contribution of water runoff to the system recharge that enters through the
291 Villaluenga del Rosario shaft, as well as slight contribution due to the measurement uncertainties.

292 To check the hydrogeological connection between direct/runoff infiltration points and the main outlets draining the
293 Ubrique aquifer, two multi-tracer field experiments were performed in 2018, with the Villaluenga del Rosario shaft
294 as the common injection point. The dye tests allowed for identification of the recharge dynamics that occur in the
295 system (Fig. 2). Additionally, maximum flow velocities were estimated, being 184 m/h for Garciago spring, 129 m/h
296 for Algarrobal spring and 178 m/h for Cornicabra spring. The tracer field experiments confirmed that the recharge of
297 the test site partly occurs in a fast and concentrated way, through several swallow holes (Figs. 1 and 2). However, this
298 recharge type has dual autogenic and allogenic contributions, with confirmed flow paths from the endorheic area
299 drained by the Villaluenga del Rosario shaft (allogenic) and other minor endorheic areas located in the Sierra del
300 Caillo (autogenic). The bare epikarst is extremely developed on most of the limestone outcrops (karrenfields), resulting
301 in non-runoff and/or concentrated recharge due to the hierarchical network of the vertical flow system.

302

303

304 **4.2 Vulnerability mapping by the COP method**

305 Figure 3 shows the resulting maps from applying the COP method in the Ubrique aquifer. The O factor reflects the
306 protective capacity of the overlying layers provided by soils (texture and thickness) and the lithology of the unsaturated
307 zone (fracturing, the thickness of each layer, and the confining conditions). In the test site, the soil layer is scarcely
308 developed and the carbonate rock is roughly homogenous and uncovered over most of the aquifer's extent. One of the
309 main challenges for mapping of the variables involved in the O factor is related to the absence of boreholes (or any
310 observation point) in the inner part of the aquifer. This issue is particularly common in mountainous karst aquifers and
311 leads to use of interpolation tools to simulate the approximate thickness of the unsaturated zone, for which the
312 uncertainty and reliability depend on the number of measurements and their spatial distribution across the study area.

313 Regarding the factor C, the individual map shows the two recharge scenarios provided by the COP method:
314 concentrated recharge through the swallow holes (scenario 1) and the diffuse recharge (scenario 2). For the detection
315 of exokarst features, aerial photos, digital terrain models, and satellite images can be used jointly with field surveys.
316 A digital elevation model (DEM) with 0.5 x 0.5 m grids and 0.1 m of vertical resolution, derived from light detection
317 and ranging data (LiDAR) captured in 2014, was obtained from public databases for this study (PNOA, 2016). The
318 DEM in raster format was corrected for no data values prior to being run in this analysis. Data correction was
319 performed by filling null data with average values from the surrounding grids by applying the moving window method.

320 In this research, ‘doline’ refers to any enclosed depression falling into defined morphometric attributes without
321 consideration of their genetic features.

322 The spatial delineation of the recharge basins of the swallow holes and sinking streams (scenario 1) should be based
323 not only on topography criteria but also on lithology, both concepts will highly condition their functionality regarding
324 concentrated recharge towards the sinking point. This explains the fact that in karst aquifers it is quite common that
325 carbonate outcrop areas, with well-developed epikarst, do not generate or develop effective run-off even for the
326 topographic basins of swallow holes due to its high permeability. These areas would be excluded from scenario 1.
327 Then, although GIS-based tools can readily calculate the drainage basins, the delimitation of the effective basin
328 requires detailed field observations and *in-situ* monitoring, particularly during the transitory activation of swallow
329 holes. In the test site, the functional recharge areas of the swallow holes were defined by *in-situ* observations during
330 heavy rain episodes because these points are activated under certain rainfall thresholds and during short time periods,
331 of 1 or 2 weeks as maximum.

332 On the other hand, to create the P factor map, the precipitation data of wet years from 4 rainfall stations from 1984 -
333 2018 were used. For this historical period, the mean annual precipitation of wet years ranges from 1,292 to 2,314 mm
334 and the average occurrence of rainy days is 88 per year.

335 The vulnerability is “High” and “Very High” in most of the recharge area (Fig. 3d). A large area is characterized as
336 “Very High” vulnerability due to the low natural protection of the karst aquifer (very low values of O factor), resulting
337 from the physical properties as well as the thickness of the layers above the saturated zone and the important role of
338 exokarst features that, in fact, are highly developed in the test site. Only in areas where carbonates are overlaid by
339 marls, and the surface flow is not drained towards swallow holes, the vulnerability class is “Low” or “Very Low”, but
340 these are very small patches and account for only small areas.

341 The statistical assessment of the results associated with the explanatory variables, done by the application of the OLS
342 regression, is shown in Table 1 and in Figure 4. In addition to the analysis of the complete database, the data were
343 distributed between the points within the swallow hole recharge areas (886 points) and outside them (10,174), to
344 determine whether there are differences in the relationship of the explanatory variables with the vulnerability index
345 COP.

346 According to the statistical assessment, the COP values in the Ubrique aquifer are mainly related to the variable
 347 associated with exokarstic modeling forms (Karst-f) and, secondly, by the variable associated with lithology (OL).
 348 However, “ly” and “zns” present a weak relationship with COP as single variables. Then, as was expected, the
 349 combination of lithology and thickness of the unsaturated zone determines the effect and weight on the vulnerability
 350 of an aquifer. On the other hand, the variability of soil does not present a significant relationship with the vulnerability
 351 index in this test site. The role of soil in the natural attenuation processes and, as a consequence, in groundwater
 352 protection, is very relevant. However, in the Ubrique aquifer, this variable shows a very low degree of development
 353 in most of the area, since it is spatially homogeneous, and has a small effect on the spatial pattern of the vulnerability
 354 index. As an additional point, the statistical analysis suggests that the strong relationship between the variable OL and
 355 the dependent COP disappears, until there is no significance, when performing the analysis with data of the
 356 watersheds, as expected. In this area, variables associated with recharge (Karst_f and Sv) have the strongest and the
 357 most significant relationship.

358

359 Table 1 Summary of the OLS regression results with respect to explanatory variables

Variable	Whole catchment area			Scenario 2 (non- swallow hole recharge area)			Scenario 1 (swallow hole recharge area)		
	Coef.	StdError	Robust_Pr	Coef.	StdError	Prob.	Coef.	StdError	Prob.
OS	-0.049	0.021	0.019	0.001	0.000	0.000*	0.136	0.045	0.002*
OL	0.366	0.010	0.000*	0.484	0.012	0.000*	0.048	0.029	0.103
ly	-0.001	0.000	0.000*	0.315	0.005	0.000*	0.000	0.000	0.936
zns	0.000	0.000	0.009*	0.000	0.000	0.967	0.001	0.000	0.000*
Karst_f	1.377	0.019	0.000*	1.299	0.010	0.000*	0.420	0.034	0.000*
Sv	0.018	0.060	0.771	0.658	0.025	0.000*	0.594	0.288	0.039
Slope	0.001	0.000	0.000*	0.000	0.000	0.004*	0.008	0.001	0.000*
P_int	0.117	0.010	0.000*	-0.035	0.004	0.000*	-0.460	0.043	0.000*
Pq	-0.002	0.000	0.000*	0.000	0.000	0.000*	0.003	0.001	0.000*

* indicates a statistically significant p-value ($p < 0.01$)

OS: soil characteristic
 OL: lithology subfactor (related to the attenuation capacity of each layer within the unsaturated zone)
 ly: lithology degree of fracturing
 zns: thickness of unsaturated zone
 Karst_f: surface karstic features, that include the distances to swallow hole within the scenario 1
 Sv: slope and vegetation characteristics
 Slope: slope in percentage
 P_int: intensity of precipitation of wet years
 Pq: annual rainfall of a historical series of wet years



360
361
362
363
364
365
366
367
368
369
370
371
372
373
374
375
376
377
378
379
380
381
382
383
384
385

4.3 Validation of the vulnerability map

In a similar framework to that used by previous research projects, discharge rates and selected hydrochemical parameters were monitored in the permanent springs as well as in the overflow points. Figure 5 displays the hydrodynamic behaviour of the two permanent outlets, plus Garciago overflow spring, in order to illustrate the functioning of the test site. Time series of spring discharge show a large variability, ranging in the case of Garciago spring from zero discharge to nearly 10 m³/s discharge after 1 day from the main precipitation event. The magnitudes of the observed flood peaks in the springs are proportional to that of the recharge and they tend to recover pre-event values once the recharge effect is finished. In general, the studied outlets show a typical karst behaviour with sudden and rapid variations of hydrodynamic responses during rainfall events, as well as a low natural attenuation capacity against the rainfall. Therefore, the results obtained from the hydrodynamic analysis suggest a well-developed conduit network that enables a rapid groundwater flow within the aquifer. According to the latter hypothesis, rainwater infiltrates into the aquifer and rapidly moves through interconnected conduits and fractures, causing increases in hydraulic pressure transference and decreases in groundwater mineralization.

The groundwater resources, drained by the springs and used for human consumption, are threatened quantitatively and qualitatively. Concerning the quantity of pumped groundwater resources intended for human consumption, the discharge rates during recession periods are almost zero in Algarrobal and zero in Garciago springs (Fig. 5). On the other hand, during flood events the water quality is impacted by high turbidity levels in the majority of karst outlets and by the relationship between turbidity and potential pollutant load. Turbidity or particle dynamics (considered as natural tracer) highlight the arrival of water from the surface and/or from dry/flooded conduits (or saturated syphons) within the aquifer system. Turbidity evolution observed in karst springs during high-flow periods shows fast increases after an intense precipitation event, with narrow peaks detected 25 hours (on average) before the peak discharge (Fig. 6; Martín-Rodríguez et al. 2019). In a similar way, the TOC and NO₃⁻ contents show rapid increases after the precipitation events due to the arrival of recently infiltrated waters in the aquifer through vertical karstic dissolution

386 conduits or fractures, which rapidly reach the saturated zone (Fig. 5). The effects of rainfall on the water mineralization
387 are noticeable after several hours. All these results denote an overall high vulnerability for the Ubrique aquifer.

388

389

390

391 Three dye tracers (pyranine, suforhodamine B and aminorhodamine G) injected into swallow holes in 2018 were
392 detected in the main outlets of the Ubrique aquifer, shown in Figure 1. The results of tracer tests (carried out in high-
393 water conditions), with a modal flow velocity ranging between 92.2 and 117.4 m/h, inferred an important degree of
394 inner karstification. These data again provide evidence to support the hypothesis of high vulnerability of the system,
395 especially when recharge water enters through the swallow holes.

396 In summary, the analyses of natural and artificial chemical constituents in the karst spring water confirm the extreme
397 vulnerability to contamination of the pilot site, which is coherent with the vulnerability map resulting from the
398 application of the COP method. However, some sectors of the aquifer surface where karrenfields are quite well
399 developed, display very high vulnerability in the areas close to swallow holes. To get a complete validation of the
400 vulnerability map, an additional dye tracer test designed specifically for validating the vulnerability related to diffuse
401 infiltration is further needed. This additional field experiment, in which fluorescent substances should be injected into
402 karrenfields and swallow holes, would allow one to confirm whether the high development of exokarst features leads
403 to a significant contribution to the concentrated recharge at depth or, by contrast, whether the vertical permeability is
404 quite limited. If the results of the proposed additional fieldwork are conclusive, it would permit a rethink and re-design
405 of the current conceptual hydrogeological model of the pilot site. In karst media, transferring improvements from
406 conceptual modeling to vulnerability assessment must be constantly conducted to enhance understanding of the
407 hydrogeological systems and better manage the water resources.

408

409 **4.4 Future perspectives: early warning systems (EWS)**

410 Within the framework of water supply protection, delineating protection zones for groundwater sources intended for
411 human consumption is a sanitary measure accepted and promoted in most water-related policies. In fact, as established

412 by the official guidance documents on the protection of groundwater used for drinking water (e.g. European
413 Commission 2007), protection zones in karst aquifers may need to be defined using vulnerability maps as the preferred
414 tools. However, groundwater protection requires not only static protection measures, but also the implementation of
415 monitoring and security systems. These procedures are designed to ensure the stability of the environmental and
416 hydrogeological conditions under which the protection perimeter was defined, in order to identify whether any changes
417 might impact (1) the vulnerability pattern and (2) the water quality. In both cases, vulnerability maps would require
418 revision to redefine perimeters and spatial criteria associated with planning. An early warning system (EWS) (Bartrand
419 et al. 2017, Grimmeisen et al. 2018) is one of the most adequate tools to ensure this regular monitoring.

420 The concept of an EWS comprises a set of strategies designed to support operational tasks in water supply systems to
421 optimize raw-water capture by predicting the arrival of low-quality karst groundwater. An EWS aims to identify and
422 reliably detect contamination episodes, and therefore facilitates the adaptation of drinking-water operational
423 procedures and water management strategies accordingly. The EWS and vulnerability assessment procedures share
424 the same hydrogeological knowledge as a basis for groundwater management and protection, and consequently a
425 stable feedback should be established between both approaches. Thus, vulnerability mapping is an essential step for
426 designing and improving an EWS and its related groundwater monitoring network techniques. Also data on natural
427 tracers recorded within the monitoring network of the EWS can help to validate the vulnerability maps.

428 In rural karst areas, such as the Ubrique test site, fecal bacteria and other pathogens often originate from farming and
429 agricultural activities, such as cattle pasturing and the application of manure (Drew and Hötzl 1999; Boyer and
430 Pasquarell 1999). These kinds of pollutants (and other inorganic substances), which pose a threat to drinking water
431 catchments, can easily enter the aquifer through preferential flow paths. Prolonged periods of good water quality may
432 thus be interrupted by short microbial contamination events. Identifying those is a major challenge in the protection
433 of karst water sources (Pronk et al. 2007). The EWS quality monitoring strategies have been presented as a promising
434 tool that can foresee and detect the effects of pollution on groundwater quality in karst aquifers intended to drinking
435 water supply of both urban and rural populations. An EWS identifies easy-to-measure parameters or combinations of
436 them that indirectly predict the possible arrival of microbial pathogens at supply points. Different approaches have
437 been selected to achieve this objective in near real-time, and which have shown a good correlation with fecal
438 contamination and microbial pathogens: turbidity (Nebbache et al. 1997; Ryan and Meiman, 1996; Massei et al. 2003),
439 organic carbon content (Pronk et al. 2005, Frank et al. 2018), spring discharge (Auckenthaler et al. 2002), particle size

440 distribution (Pronk et al. 2007; Goldscheider et al. 2010), and other indirect methods, like the measurement of the
441 enzymatic activity (Ryzinska-Paier et al. 2014; Ender et al. 2017), fluorescence-based techniques (Frank et al. 2018)
442 or tryptophan-like fluorescence (Mudarra et al. 2011; Sorensen et al. 2015).

443 Water drained by Ubrique aquifer springs (Cornicabra, Algarrobal and Garciago) is used for drinking water purposes.
444 The spring waters suffer frequent pollution episodes, in which high loads of inorganic sediment particles and bacteria
445 arise during stormy rainfall events (Sánchez et al. 2017; Martín-Rodríguez et al. 2019). These events of high turbidity
446 affect the exploitation of the available water resources, since during these conditions it is not possible to capture pristine
447 groundwater and use it for water supply. Under these circumstances, the implementation of an EWS is an unique
448 opportunity for safeguarding water quality.

449 The procedure for the implementation of the EWS at Ubrique test site consists of three phases for its full execution
450 (Fig. 7): (1) continuous monitoring of the natural responses of the springs, including both easy-to-measure (discharge,
451 electrical conductivity, water temperature and turbidity) and novel (DOM, TOC, tryptophan, *E. Coli* and particle size
452 distribution) parameters; (2) analysis of short/long-term data series and application of properly adapted artificial neural
453 network (ANN)-based algorithms (Zhang et al. 2018) to identify the presence of microbial pathogens for their indirect
454 detection from easy-to-measure *in-situ* parameters and to forecast water quality based in meteorological predictions;
455 (3) system launch with an operational perspective, and the assessment of selected operational key performance
456 indicators (KPIs) for EWS optimal performance. These KPIs are statistical metrics used to gain insights into the
457 efficiency and productivity of the measurement strategies carried out to optimize user-defined operational protocols.
458 Phase 1 allows one to acquire records of physico-chemical water parameters, together with dye test performance data,
459 to get a full picture of the system dynamics. By the application of algorithms based on ANN, using as inputs the
460 database acquired in phase 1, the combination of parameters that most accurately indicates the presence of microbial
461 pathogens will be identified. The ANN approach for better predictions of microbiological contamination events based
462 on near real-time multi-parameter monitoring has been successfully used for EWS of water quality (e.g. Zhang et al.
463 2018).

464 Finally, in the operational phase, the information provided by the easy-to-measure recording probes for real-time
465 monitoring and meteorological predictions will be transferred online to a web database. Based on the hydrological
466 and hydrochemical monitoring data, the algorithm continuously assesses the potential risk of a contamination event

467 occurring and automatically validates its forecasting in near real time (hourly resolution), to give a warning about the
468 risk of contamination for spring water quality (Grimmeisen et al. 2018, Zhang et al. 2019). Consequently, the water
469 company operator could be assisted by the system in terms of operational works. The system alerts the drinking water
470 suppliers when the performance algorithm reaches a critical threshold. The optimization process will be continuous,
471 as the system gets a feedback from the analysis of data acquired on each contamination event, which will permit a
472 continuous optimization in system performance from the analysis of selected KPIs.

473

474

475 **5 Challenges in karst groundwater vulnerability mapping**

476 Methods of groundwater vulnerability mapping in karst aquifers have progressed in the last 20 years, being solid,
477 useful and effective tools in the protection of water resources. Groundwater vulnerability assessment methods have
478 been developed as the necessary basis for implementing groundwater protection measures, with the delimitation of
479 protection zones being one of the most relevant tools. However, as mentioned in previous sections, given that the
480 vulnerability to contamination is not empirically quantified, but rather requires a modeling and simplification of
481 hydrogeological characteristics, vulnerability mapping and assessment are not exempt from uncertainties, and integral
482 water supply protection is still a challenging issue. Among the most relevant challenges that researchers will have to
483 deal with in the near future are:

- 484 1. The development of protocols and tools that strengthen the decision tree during the implementation of the
485 methodologies, as well as the validation of the results. Vulnerability mapping has become a routine procedure
486 to support land-use planning as a measure to protect groundwater quality; the validation of vulnerability maps
487 and protection zoning is essential for proper land-use planning and for understanding what is really meant by
488 the vulnerability degree shown on the map. Validation may be undertaken by analysis of the hydrodynamic
489 and hydrochemical responses of the main springs, combined with analysis of the temporal evolution of
490 natural tracers of infiltration and complementary dye tracer tests that must be specifically designed to check
491 the vulnerability to pollution (Marin et al. 2015). A good knowledge of hydrogeological functioning and karst
492 behavior constitutes a complementary procedure that feeds back into the vulnerability mapping exercise
493 (Marin et al. 2015, Kazakis et al. 2018). Thus, the hydrogeological characterization should not be the end in

494 itself, but a way to assess the vulnerability of groundwater to contamination, and the validation of
495 vulnerability can contribute to extending knowledge about the karst aquifer. This symbiotic relationship also
496 occurs between the EWS and vulnerability mapping, where the results of the latter help to design the EWS
497 monitoring network, at the same time that chemographs will allow a better interpretation of the system
498 functioning and, therefore, a readjustment, in a feedback manner, of those parameters that should be involved
499 in the assessment.

500 2. Groundwater exploitation and contamination have become of global concern (Gregory et al. 2013; Zheng
501 and Liu 2013). A suitable groundwater protection strategy requires the conceptualization of the
502 hydrogeological functioning for system characterization. The proper protection of karst groundwater
503 becomes a difficult task in developing countries where important gaps in hydrogeological knowledge exist
504 for vast regions (Taheri et al 2015). Therefore, the availability of consistent water-related databases and
505 approaches, and their validation and interpretation, are of utmost importance for complex hydrogeological
506 systems such as karst aquifers. This situation stimulates a demand for establishing flexible and simplified
507 methods that could be applied with the least available data and still lead to acceptable interpretations.
508 However, this simplification needs to be addressed carefully since vulnerability mapping in karst can result
509 in a considerably large degree of uncertainty. As mentioned previously, this uncertainty could be
510 unmanageable, resulting in a poor assessment and incorrect evaluation. For relevant countries, since the
511 Sustainable Development Goal 6 (SDG6) of the United Nations (UN-Water 2018) aims to ensure availability
512 and sustainable management of water and sanitation for all, a strong commitment of local and international
513 organizations with experience in the research and protection of groundwater are necessary, as a long-term
514 prospect.

515 3. In the climate change context, the predicted changes, such as an increase in the frequency of extreme drought
516 in the Mediterranean domain or increase of extreme precipitation events in the Atlantic and Boreal
517 biogeographical regions (EEA 2017), will affect the current hydrogeological balance and the trade-off of
518 water supplies for different end-users. Some research has shown that the flood pulses caused by precipitation
519 events after a long dry period cause a significant deterioration in water quality, with a significant increase of
520 turbidity, as occurs in Ubrique springs, and even in the amount of coliform bacteria in the water (Ravbar et
521 al. 2018). Therefore, the proper identification of the vulnerable zones of recharge areas becomes even more

522 relevant, at the same time that the implementation of EWS will be an increasingly necessary management
523 and control tool for continuous monitoring of the karst water quality to ensure safe quality. Further work
524 needs to be done to simulate site-specific hydraulic responses to different climate scenarios, and there needs
525 to be further thought on how to adapt water management and protection plans towards an increase in the
526 resilience of water supply that supports the local population.

527

528 **6 Conclusions**

529 Karst aquifers are highly sensitive to the effects of contamination, and priority must be given to contamination
530 prevention for the sustainability of groundwater resources. This work, which has a groundwater vulnerability
531 perspective and a purely hydrogeological focus, provides evidence (supporting previous work) that karst aquifers
532 require the development of common groundwater protection strategies, resulting in integrated management plans
533 based on the continuous processes of feedback and re-evaluation of the system function and protection criteria
534 (Kazakis et al. 2018). In the case of the test site, the characterized karst behavior and conduit flow system, and the
535 significant contribution of the allogenic component to the total recharge of the aquifer, permit the mobilization of
536 contaminants originating from livestock in the surrounding areas and from partially treated waste water, as well as
537 inorganic sediment particles when stormy rainfall events occur. Consequently, the protection of groundwater and the
538 preventive principles must be considered as the appropriate strategies to minimize the water pollution risk and the
539 potentially negative effects on human health.

540 The work presented here is part of a broader project that includes the implementation of an EWS, addressing an
541 integrated protection and management strategy for the Ubrique aquifer. Considerable progress has been made, but
542 advances are still necessary due to the hydrological complexity of the karst aquifers here. Ongoing investigations,
543 whose initial phases are presented in this work, should trigger the implementation of tools for comprehensive and safe
544 management of the karst groundwater resources. Despite its humid climate, having precipitation much higher than
545 that of the rest of the Andalusia region of Spain, and even at country level, the rainfall regime at the study area is also
546 threatened in the future projections associated with climate change. The delineation of the protection zones of the karst
547 springs (Cornicabra and Algarrobal) used for water supply, based on vulnerability mapping and land-use management
548 policies, and the operational implementation of an EWS in the captured points for potable use, will mean advances in

549 the management of the water supply, including enhanced safety and resilience for the water supply to the nearby rural
550 municipalities.

551 This research links different methods applied to the protection of the source from contamination events. The methods
552 range from classical hydrodynamic and hydrochemical approaches, to the implementation of protection zones and
553 early warning groundwater quality monitoring networks. Such a combined application allows a deeper understanding
554 of contaminant transport in karst aquifers, natural attenuation processes, transit times, and the influence of these factors
555 on other water parameters. For the development and implementation of an EWS for karst springs, it is necessary to
556 have a solid understanding of the hydrogeological functioning of the whole aquifer, particularly with regard to
557 groundwater vulnerability to pollution. EWSs have become a promising integrated monitoring tool for practical
558 application of vulnerability maps, focusing on the source protection. A double-sense feedback is established between
559 both tools: on one hand, vulnerability mapping is an essential step for an optimal design of the EWS and its related
560 groundwater monitoring network techniques (providing continuous feedback from data gathering), as well as
561 identifying potentially hazardous human activities which could rapidly change the chemical and microbial quality of
562 the groundwater. On the other hand, continuous validation of vulnerability maps can be achieved through the data
563 analysis of natural and/or anthropogenic-induced tracers recorded by the spring monitoring network. The acquired
564 knowledge of solute transport in the groundwater, and its reactivity, also allows for testing the accuracy of the
565 selected vulnerability mapping approach. The use of dye tracers specifically planned to validate vulnerability mapping
566 are highly recommended to assess the accuracy of the selected vulnerability mapping approach as well as be also
567 useful for EWS delineation.

568

569 **Acknowledgments**

570 This work has been developed under the Research Group RNM-308 of Junta de Andalucía. It is a contribution to the
571 European Project “Karst Aquifer Resources availability and quality in the Mediterranean Area (KARMA)” PRIMA,
572 ANR-18-PRIM-0005; the associated project PCI2019-103675 funded by the Spanish Research Agency through the
573 scientific programme “Programación Conjunta Internacional”. Additionally, it contributes to the project PID2019-
574 111759RB-I00 funded by the Autonomous Government of Andalusia (Spain), with support of the Environmental and
575 Water Agency of Andalusia. The authors thank the local government of Ubrique village and water managers for their

576 collaboration. Finally, we want to acknowledge the associate editor and anonymous reviewers for their constructive
577 comments, which contributed to improving the manuscript.

578

579

580 **References**

581 Andreo B, Goldscheider N, Vadillo I, Vías JM, Neukum C, Sinreich M, Jiménez P, Brechenmacher J, Carrasco F,
582 Hötzl H, Perles JM, Zwahlen F (2006) Karst groundwater protection: first application of a Pan-European
583 approach to vulnerability, hazard and risk mapping in the Sierra de Líbar (southern Spain), *Sci. Total Environ.*
584 357(1-3):54–73, doi 10.1016/j.scitotenv.2005.05.019

585 Andreo B, Ravbar N, Vías JM (2009) Source vulnerability mapping in carbonate (karst) aquifers by extension of the
586 COP method: application to pilot sites, *Hydrogeol J.* 17(3):749–758, doi 10.1007/s10040-008-0391-1

587 Andreo B, Sánchez D, Martín-Algarra A (2014) Caracterización hidrogeológica y evaluación de los recursos hídricos
588 de la Sierra de Grazalema (Cádiz) para su potencial implementación como reserva estratégica de agua en la
589 cabecera de la Demarcación Hidrográfica del Guadalete-Barbate (Hydrogeological characterization and
590 evaluation of the water resources of the Sierra de Grazalema (Cádiz) for potential implementation as a strategic
591 water reserve at the head of the Guadalete-Barbate Hydrographic Demarcation). Andalusian Water Agency
592 Technical report, Spain, p 128

593 Auckenthaler A, Raso G, Huggenberger P (2002) Particle transport in a karst aquifer: natural and artificial tracer
594 experiments with bacteria, bacteriophages and microspheres, *Water Sci Technol* 46(3):131–138, doi
595 10.2166/wst.2002.0072

596 Bakalowicz M (2005) Karst groundwater: A challenge for new resources. *Hydrogeol J.* 13:148–160.

597 Barberá JA, Andreo B (2012) Functioning of a karst aquifer from S Spain under highly variable climate conditions,
598 deduced from hydrochemical records, *Environ Earth Sci*, 65(8):2337–49, doi 10.1007/s12665-011-1382-4

599 Barberá JA, Mudarra M, Andreo B, De la Torre B (2018) Regional-scale analysis of karst underground flow deduced
600 from tracing experiments: examples from carbonate aquifers in Malaga province, southern Spain,
601 *Hydrogeology J.* 26(1):23-40, doi 10.1007/s10040-017-1638-5

602 Bartrand T, Grayman W, Haxton T (2017) Drinking Water Treatment Source Water Early Warning System State of
603 the Science Review. U.S. Environmental Protection Agency, Washington, DC, EPA/600/R-17/405.

604 Batiot C, Liñán C, Andreo B, Emblanch C, Carrasco F, Blavoux B (2003) Use of TOC as tracer of diffuse infiltration
605 in a dolomitic karst system: the Nerja Cave (Andalusia, southern Spain), *Geophys Res Lett* 30(22):2179, doi
606 10.1029/2003GL018546.

607 Boyer DG, Pasquarell GC (1999) Agricultural land use impacts on bacterial water quality in a karst groundwater
608 aquifer, *J Am Water Resou Assoc* 35(2):291–300, doi 10.1111/j.1752-1688.1999.tb03590.x

609 Butscher C, Huggenberger P (2008) Intrinsic vulnerability assessment in karst areas: A numerical modeling approach,
610 *Water Resour. Res.*, 44(3):W03408, doi 10.1029/2007WR006277

611 Celle-Jeanton H, Travy Y, Blavoux B (2001) Isotopic typology of the precipitation in the Western Mediterranean
612 region at three different time scales, *Geophysical Research Letters*, 28(7):1215–1218, doi
613 10.1029/2000GL012407

614 Daly C, Gibson WP, Taylor GH, Johnson GL, Pasteris P (2002) A knowledge-based approach to the statistical
615 mapping of climate, *Clim Res* 22(2):99-113, doi 10.3354/cr022099

616 Delannoy JJ (1987) Reconocimiento biofísico de Espacios Naturales de Andalucía [Biophysical survey of the natural
617 spaces of Andalusia]. Junta de Andalucía, Madrid.

618 Doerfliger N, Zwahlen F (1998) Practical guide, groundwater vulnerability mapping in karstic regions (EPIK). Swiss
619 Agency for the Environment, Forests and Landscape (SAEFL), Bern. p 56

620 Drew D, Hötzl H (eds) (1999) *Karst Hydrogeology and Human Activities. Impacts, Consequences and Implications—*
621 *International Contributions to hydrogeology*, 20. Balkema, Rotterdam. p 338

622 EEA, European Environment Agency (2017) *Climate change, impacts and vulnerability in Europe 2016. An indicator-*
623 *based report.* EEA Report No 1/2017. doi:10.2800/534806

624 Ender A, Goeppert N, Grimmeisen F, Goldscheider N (2017) Evaluation of β -D-glucuronidase and particle-size
625 distribution for microbial water quality monitoring in Northern Vietnam, *Sci. Total Environ.* 580:996–1006,
626 doi 10.1016/j.scitotenv.2016.12.054

627 European Commission (2007) *Common implementation strategy for the Water Framework Directive (200/60/EC),*
628 *Guidance Document No. 16 on Groundwater in Drinking Water Protected Areas.* European Commission,
629 Brussels.

630 Ford D, Williams PD (2007) *Karst Hydrogeology and Geomorphology.* John Wiley & Sons Ltd., Chippenham,
631 Wiltshire, UK.

632 Foster S (1987) Fundamental concepts in aquifer vulnerability, pollution risk and protection strategy. In: Van
633 Duijvenbooden,W., VanWaegeningh, H.G. (Eds.), *Vulnerability of Soil and Groundwater to Pollutants* 38.
634 TNO Committee on hydrological research, pp. 69–86.

635 Foster S, Hirata R, Andreo B (2013) The aquifer pollution vulnerability concept –aid or impediment in promoting
636 groundwater protection? *Hydrogeol J.* 21(7):1389-1392, doi 10.1007/s10040-013-1019-7

637 Frank S, Goeppert N, Goldscheider N (2018) Fluorescence-based multi-parameter approach to characterize dynamics
638 of organic carbon, faecal bacteria and particles at alpine karst springs, *Sci. Total Environ.* 615:1446-1459, doi
639 10.1016/j.scitotenv.2017.09.095

640 Genthon P, Bataille A, Fromant A, D’Hulst D, Bourges F (2005) Temperature as a marker for karstic waters
641 hydrodynamics. Inferences from 1 year recording at La Peyrère cave (Ariège, France), *J Hydrol* 311(1-4):157–
642 171, doi 10.1016/j.jhydrol.2005.01.015

643 Ghasemizadeh R, Yu X, Butscher C, Padilla IY, Alshawabkeh A (2016) Improved regional groundwater flow
644 modeling using drainage features: a case study of the central northern karst aquifer system of Puerto Rico
645 (USA), *Hydrogeol J.* 24(6):1463–1478, doi 10.1007/s10040-016-1419-6

646 Gogu RC, Hallet V, Dassargues A (2003) Comparison of aquifer vulnerability assessment techniques: application to
647 the Neblon river basin (Belgium), *Environ Geol* 44(8):881–892, doi 10.1007/s00254-003-0842-x

648 Gogu RD, Dassargues A (2000) Sensitivity analysis for the EPIK method of vulnerability assessment in a small karstic
649 aquifer, southern Belgium. *Hydrogeol J.* 8(3):337–345, doi 10.1007/s100400050019

650 Goldscheider N, Klute M, Sturm S, Hötzl H (2000) The PI method: a GIS based approach to mapping groundwater
651 vulnerability with special consideration of karst aquifers, *Z Angew Geol*, 46(3):157–66

652 Goldscheider N (2005) Karst groundwater vulnerability mapping: application of a new method in the Swabian Alb,
653 Germany, *Hydrogeol J.* 13(4):555–564, doi 10.1007/s10040-003-0291-3

654 Goldscheider N, Drew D (eds) (2007) *Methods in karst hydrogeology. International Contribution to Hydrogeology,*
655 IAH, vol 26. Taylor and Francis/Balkema, London.

656 Goldscheider N, Meiman J, Pronk M, Smart C (2008) Tracer tests in karst hydrogeology and speleology, *Int. J. Spel.*
657 37(1):27–40, doi doi.org/10.5038/1827-806X.37.1.3

658 Goldscheider N, Pronk M, Zopfi J (2010) New insights into the transport of sediments and microorganisms in karst
659 groundwater by continuous monitoring of particle size distribution, *Geol. Croat.* 63(2):137–142, doi
660 10.4154/gc.2010.10

661 Goldscheider N, Chen Z, Auler AS, Bakalowicz M, Broda S, Drew D, Hartmann J, Jiang G, Moosdorf N, Stevanovic
662 Z, Veni G (2020) Global distribution of carbonate rocks and karst water resources. *Hydrogeol J* 28, 1661–1677.
663 <https://doi.org/10.1007/s10040-020-02139-5>

664 Gregory JM, Whiteb NJ, Churchb JA, Bierkensc MFP, Boxd JE, van den Broekee MR, Cogleyf JG, Fettweisg X,
665 Hannah E, Huybrechtsi P, Konikowj LF, Leclercq PW, Marzeionk B, Oerlemanse J, Tamisieal ME, Wadam
666 Y, Waken LM, van de Wale RSW (2013) Twentieth-century global-mean sea level rise: Is the whole greater
667 than the sum of the parts?, *J. Clim.* 26(13):4476–4499, doi:10.1175/JCLI-D-12-00319.1

668 Grimmeisen F, Riepl D, Schmidt S, Xanke J, Goldscheider N (2018) Set-up of an early warning system for an
669 improved raw water management of karst groundwater resources in the semi-arid side Wadis of the Jordan
670 Valley, *Geophysical Research Abstracts*, Vol. 20, EGU2018-16731, EGU General Assembly

671 Hargreaves GH, Samani ZA (1985) Reference crop evapotranspiration from temperature. *Transaction of ASAE*
672 1(2):96-99.

673 Hartmann A, Barberá JA, Lange J, Andreo B, Weiler M (2013) Progress in the hydrologic simulation of time variant
674 recharge areas of karst systems - Exemplified at a karst spring in Southern Spain, *Advances in Water Resources*,
675 54:149–160, doi 10.1016/j.advwatres.2013.01.010

676 Hartmann A, Goldscheider N, Wagener T, Lange J, Weiler M (2014) Karst water resources in a changing world:
677 Review of hydrological modeling approaches, *Reviews of Geophysics*, 52(3):218–242, doi
678 10.1002/2013RG000443

679 Hunkeler D, Mudry J (2007) Hydrochemical methods, in: Goldscheider, N., Drew, D. (Eds.) *Methods in karst*
680 *hydrogeology*. Taylor & Francis/Balkema, London, UK, pp. 93-121.

681 Jeannin PY, Eichenberger U, Sinreich M, Vouillamoz J, Malard A, Weber E (2013) KARSYS: a pragmatic approach
682 to karst hydrogeological system conceptualisation. Assessment of groundwater reserves and resources in
683 Switzerland, *Environ. Earth Sci.* 69(3):999–1013, doi 10.1007/s12665-012-1983-6

684 Katsanou K, Lambrakis N (2017) First outcomes of the cop method application for the assessment of intrinsic
685 vulnerability of in the karst system of Vouraikos catchment, Greece, *Journal of Earth Sciences &*
686 *Environmental Studies*, 3(1): 324-331, doi 10.25177/JESES.3.1.1

687 Kavouri K, Plagnes V, Tremoulet J, Dörfliger N, Fayçal R, Marchet P (2011) PaPRIKa: a method for estimating karst
688 resource and source vulnerability—application to the Ouyse karst system (southwest France), *Hydrogeol J.*
689 19(2):339–353, doi 10.1007/s10040-010-0688-8

690 Kazakis N, Chalikakis K, Mazzilli N, Ollivier C, Manakos A, Voudouris K (2018) Management and research strategies
691 of karst aquifers in Greece: literature overview and exemplification based on hydrodynamic modelling and
692 vulnerability assessment of a strategic karst aquifer. *Sci Total Environ.* 643, 592-609. DOI:
693 10.1016/j.scitotenv.2018.06.184

694 Margat J (1968) *Vulnérabilité des nappes d’eau souterraine à la pollution: Bases de la cartographie: Orléans, France*
695 *(Vulnerability of groundwater to pollution: Basis of mapping: Orléans, France)*, Bureau de Recherche
696 *Géologique et Minière, Document 68 SGL 198 HYD*

697 Marín AI, Dörfliger N, Andreo B (2012) Comparative application of two methods (COP and PaPRIKa) for
698 groundwater vulnerability mapping in Mediterranean karst aquifers (France and Spain), *Environ. Earth Sci.*
699 65(8):2407–2421, doi 10.1007/s12665-011-1056-2

700 Marín AI, Andreo B (2015) Vulnerability to Contamination of Karst Aquifers. In: Stevanović Z. (eds) *Karst*
701 *Aquifers—Characterization and Engineering. Professional Practice in Earth Sciences.* Springer, Cham. pp 251-
702 266, doi 10.1007/978-3-319-12850-4_8

703 Marin AI, Andreo B, Mudarra M (2015) Vulnerability mapping and protection zoning of karst springs. Validation by
704 multitracer tests, *Sci. Total Environ*, 532:435–446, doi 10.1016/j.scitotenv.2015.05.029

705 Martín-Algarra M (1987) *Evolución geológica alpina del contacto entre las Zonas Internas y Externas de la Cordillera*
706 *Bética (Alpine geological evolution of the contact between the Internal and External Zones of the Betic*
707 *Cordillera)*. PhD Thesis, University of Granada, Spain. p 1171

708 Martín-Rodríguez JF, Sánchez D, Mudarra M, Andreo B, López-Rodríguez M, Navas-Gutiérrez MR (2016)
709 *Evaluación de recursos hídricos y balance hidrogeológico en acuíferos kársticos de montaña. Caso de la Sierra*
710 *de Grazalema (Cádiz, España) (Evaluation of the water resources and hydrogeological balance in mountain*
711 *karst aquifers. Case of the Sierra de Grazalema (Cádiz, Spain))*. In: *Las aguas subterráneas y la planificación*

712 hidrológica (Groundwater and hydrological planning). Spanish-Portuguese Congress. IAH Spanish Chapter.
713 Madrid (Spain), November 2016. pp 163-170

714 Martín-Rodríguez JF, Mudarra M, Andreo B, Sánchez D (2019) Analysis of the water turbidity in karst springs from
715 S Spain and its relationship with other natural responses, Poster at 46th IAH Congress - Malaga, Spain 2019,
716 Contribution ID: 712

717 Massei N, Wang HQ, Dupont JP, Rodet J, Laignel B (2003) Assessment of direct transfer and resuspension of particles
718 during turbid floods at a karstic spring, *J. Hydrol.* 275(1-2):109–121, doi 10.1016/S0022-1694(03)00020-9

719 Mayaud C, Wagner T, Benischke R, Birk S (2014) Single event time series analysis in a binary karst catchment
720 evaluated using a groundwater model (Lurbach system, Austria). *J Hydrol.* 511:628-639.
721 <http://dx.doi.org/10.1016/j.jhydrol.2014.02.024>

722 Mudarra M, Andreo B. (2011) Relative importance of the saturated and the unsaturated zones in the hydrogeological
723 functioning of karst aquifers. The case of Alta Cadena (Southern Spain). *J Hydrol*, 397(3-4):263-280.

724 Mudarra M, Andreo B, Barberá JA, Mudry J (2014) Hydrochemical dynamics of TOC and NO₃⁻ contents as natural
725 tracers of infiltration in karst aquifers, *Environ. Earth Sci*, 71(2):507-523, doi 10.1007/s12665-013-2593-7.

726 Mudarra M, Andreo B, Baker A (2011) Characterisation of dissolved organic matter in karst spring waters using
727 intrinsic fluorescence: relationship with infiltration processes. *Sci. Total Environ.* 409(18):3448–3462, doi
728 10.1016/j.scitotenv.2011.05.026

729 Mudarra M, Hartmann A, Andreo B (2019) Combining Experimental Methods and Modeling to Quantify the Complex
730 Recharge Behavior of Karst Aquifers. *Water Resour. Res.*, 55(2):1384-1404, doi 10.1029/2017WR021819

731 Mudry J (1987) Apport du traçage physico–chimique naturel à la connaissance hydrocinématique des
732 aquifères carbonatés (Contribution of natural physico-chemical tracing to the hydrokinematic knowledge of
733 carbonated aquifers). PhD thesis, University of Franche-Comté. p 400

734 Nebbache S, Loquet M, Vincelas-Akpa M, Feeny V (1997) Turbidity and microorganisms in a karst spring. *Eur. J.*
735 *Soil Biol.* 33:89–103

736 Neukum C, Hötzl H (2007) Standardization of vulnerability maps. *Environ Geol* 51(5):689–694, doi 10.1007/s00254-
737 006-0380-4

738 Perrin J, Jeannin PY, Cornaton F (2007) The role of tributary mixing in chemical variations at a karst spring, Milandre,
739 Switzerland, *J. Hydrol.* 332(1-2):158–173, doi 10.1016/j.jhydrol.2006.06.027

740 Perrin J, Pochon A, Jeannin P, Zwahlen F (2004) Vulnerability assessment in karstic areas: validation by field
741 experiments, *Environ. Geol.* 46(2):237–245, doi 10.1007/s00254-004-0986-3

742 Polemio M, Casarano D, Limoni PP (2009) Karstic aquifer vulnerability assessment methods and results at a test site
743 (Apulia, southern Italy), *Nat Hazards Earth Syst Sci*, 9(4):1461–1470, doi 10.5194/nhess-9-1461-2009

744 PNOA (2016) –PNOA LiDAR. Instituto Geográfico Nacional, Gobierno de España PNOA (Plan Nacional de
745 Ortofotografía Aérea). <http://pnoa.ign.es/presentacion-y-objetivo> [accessed: December 23, 2016].

746 Pronk M, Goldscheider N, Zopfi J (2005) Dynamics and interaction of organic carbon, turbidity and bacteria in a karst
747 aquifer system, *Hydrogeol. J.* 14(4):473–484, doi 10.1007/s10040-005-0454-5

748 Pronk M, Goldscheider N, Zopfi J (2007) Particle-size distribution as indicator for faecal bacteria contamination of
749 drinking water from karst springs, *Environ. Sci. Technol.* 41(24):8400–8405, doi 10.1021/es071976f

750 Ravbar N, Goldscheider N (2007) Proposed methodology of vulnerability and contamination risk mapping for the
751 protection of karst aquifers in Slovenia, *Acta Carsologica* 36(3):461–475, doi 10.3986/ac.v36i3.174

752 Ravbar N, Goldscheider N (2009) Comparative application of four methods of groundwater vulnerability mapping in
753 a Slovene karst catchment, *Hydrogeol J.* 17(3):725–733, doi 10.1007/s10040-008-0368-0

754 Ravbar N, Kovačič G, Petrič M, Kogovšek J, Brun C, Koželj A (2018) Climatological trends and anticipated karst
755 spring quantity and quality: case study of the Slovene Istria. In: Parise M, Gabrovsek F, Kaufmann G, Ravbar
756 N (eds) *Advances in Karst Research: Theory, Fieldwork and Applications*. Geological Society, London,
757 Special Publications, 466, 295-305. First published online November 28, 2017, doi 10.1144/SP466.19

758 RD 140/2003. Real Decreto-ley de 7 de febrero, por el que se establecen los criterios sanitarios de la calidad del agua
759 de consumo humano (Royal Decree of 7 February, which establishes the sanitary criteria for the quality of
760 water for human consumption). *Boletín Oficial del Estado*, 21 de febrero de 2003, núm. 45, pp. 7228-7245.

761 Ryan M, Meiman J (1996) An examination of short-term variations in water quality at a karst spring in Kentucky.
762 *Ground Water* 34(1):23–30, doi 10.1111/j.1745-6584.1996.tb01861.x

763 Ryzinska-Paier G, Lendenfeld T, Correa K, Stadler P, Blaschke AP, Mach RL, Stadler H, Kirschner AKT, Farnleitner
764 AH (2014) A sensitive and robust method for automated on-line monitoring of enzymatic activities in water
765 and water resources. *Water Sci. Technol* 69(6):1349–1358, doi 10.2166/wst.2014.032

766 Sánchez D, Barberá JA, Mudarra M, Andreo B, Martín JF (2018) Hydrochemical and isotopic characterization of
767 carbonate aquifers under natural flow conditions, Sierra Grazalema Natural Park, southern Spain In: Parise M,

768 Gabrovsek F, Kaufmann G, Ravbar N (eds) *Advances in Karst Research: Theory, Fieldwork and Applications*.
769 Geological Society, London, Special Publications 466, 275–293. First published online November 28, 2017,
770 <https://doi.org/10.1144/SP466.16>

771 Sánchez D, Barberá JA, Mudarra M, Andreo B (2017) Hydrogeochemical tools applied to the study of carbonate
772 aquifers: examples from some karst systems of southern Spain, *Environ Earth Sci*, 74(1):199–215, doi
773 10.1007/s12665-015-4307-9

774 Sánchez D, Martín-Rodríguez JF, Mudarra M, Andreo B, López M. Navas MR (2016) Time-lag analysis of natural
775 responses during unitary recharge events to assess the functioning of carbonate aquifers in Sierra de Grazalema
776 Natural Park (Southern Spain), *Eurokarst 2016*, Neuchâtel, pp 157-167, ISBN:978-3-319-45465-8.

777 Shuster ET, White WB (1971) Seasonal fluctuations in the chemistry of limestone springs: A possible means for
778 characterizing carbonate aquifers, *J. Hydrol*, 14:93-128, doi:10.1016/0022-1694(71)90001-1

779 Sorensen JPR, Lapworth DJ, Marchant BP, Nkhuwa DCW, Pedley S, Stuart ME, Bell RA, Chirwa M, Kabika J,
780 Liemisa M, Chibesa M, (2015) In-situ tryptophan-like fluorescence: a real-time indicator of faecal
781 contamination in drinking water supplies, *Water Res.* 81, 38–46, doi 10.1016/j.watres.2015.05.035

782 Stevanović Z (2015) *Karst Aquifers – Characterization and Engineering*. Springer, Cham, Switzerland. p 692

783 Taheri K, Taheri M, Mohsenipour F (2015) LEPT, a simplified approach for assessing karst vulnerability in regions
784 by sparse data: a case in Kermanshah province, Iran. 14th Sinkholes and the Engineering and Environmental
785 Impacts of Karst: Proceedings of the Fourteenth Multidisciplinary Conference, doi
786 10.5038/9780991000951.1032

787 Turk J, Malard A, Jeannin PY, Petrič M, Gabrovšek F, Ravbar N, Vouillamoz J, Slabe T, Sordet V (2014)
788 Hydrogeological characterization of groundwater storage and drainage in an alpine karst aquifer (the Kanin
789 massif, Julian Alps), *Hydrol. Process.* 29:1986– 1998, doi 10.1002/hyp.10313

790 UN-WATER, (2018) Sustainable Development Goal 6, Synthesis Report on Water and Sanitation. United Nations –
791 Water.
792 [https://www.unwater.org/app/uploads/2018/12/SDG6_SynthesisReport2018_WaterandSanitation_04122018.](https://www.unwater.org/app/uploads/2018/12/SDG6_SynthesisReport2018_WaterandSanitation_04122018.pdf)
793 pdf

794 Vías JM, Andreo B, Perles MJ, Carrasco F (2005) A comparative study of four schemes for groundwater vulnerability
795 mapping in a diffuse flow carbonate aquifer under Mediterranean climatic conditions. *Environ Geol*,
796 47(4):586–595, doi 10.1007/s00254-004-1185-y

797 Vías J, Andreo B, Perles M, Carrasco F, Vadillo I, Jiménez P (2006) Proposed method for groundwater vulnerability
798 mapping in carbonate (karstic) aquifers: the COP method. *Hydrogeol J* 14(6):912–925

799 Vías JM, Andreo B, Ravbar N, Hötzl H (2010) Mapping the vulnerability of groundwater to the contamination of four
800 carbonate aquifers in Europe. *J Environ Manage* 91(7):1500–1510, doi 10.1007/s10040-006-0023-6

801 Yildirim M, Topkaya B (2007) Groundwater protection: a comparative study of four vulnerability mapping methods.
802 *CLEAN—Soil, Air, Water Pollution* 35(6):594–600, doi 10.1002/clen.200700144

803 Zaporozec A (1994) Concept of groundwater vulnerability. In: Vrba J, Zaporozec A (eds) *Guidebook on mapping*
804 *groundwater vulnerability. International contributions to hydrogeology*, vol 16. Verlag Heinz Heise, Hannover,
805 pp 3–8

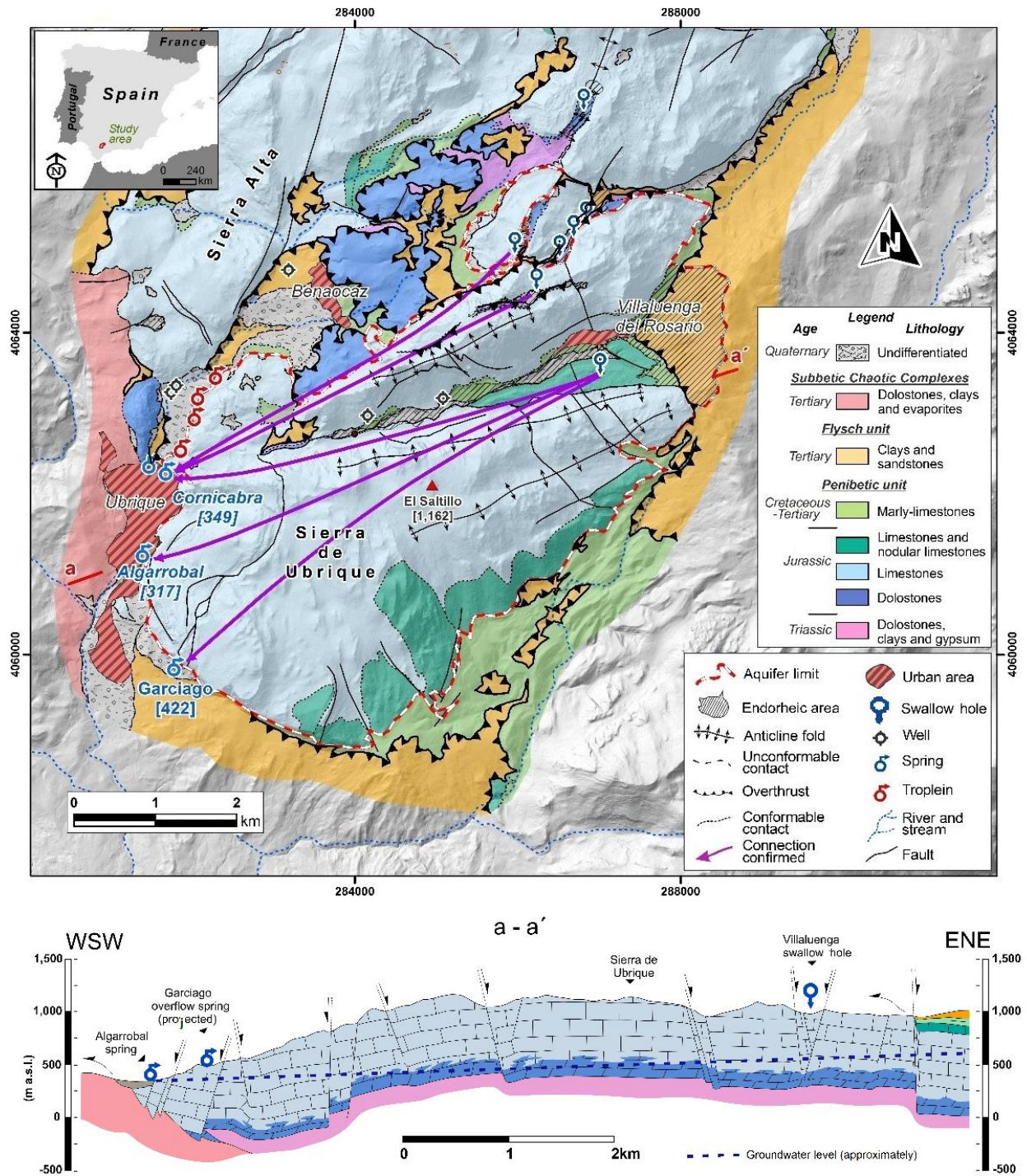
806 Zhang J, Qiu H, Li X, Niu J, Nevers MB, Hu X, Phanikumar MS (2018) Real-Time Nowcasting of Microbiological
807 Water Quality at Recreational Beaches: A Wavelet and Artificial Neural Network-Based Hybrid Modeling
808 Approach, *Environ. Sci. Technol* , 52(15), 8446-8455, doi 10.1021/acs.est.8b01022

809 Zhang Y, Gao X, Smith K, Inial G, Liu S, Conil LB, Pan B (2019) Integrating water quality and operation into
810 prediction of water production in drinking water treatment plants by genetic algorithm enhanced artificial
811 neural network, *Water Res.* 164, 0043-1354, doi 10.1016/j.watres.2019.114888

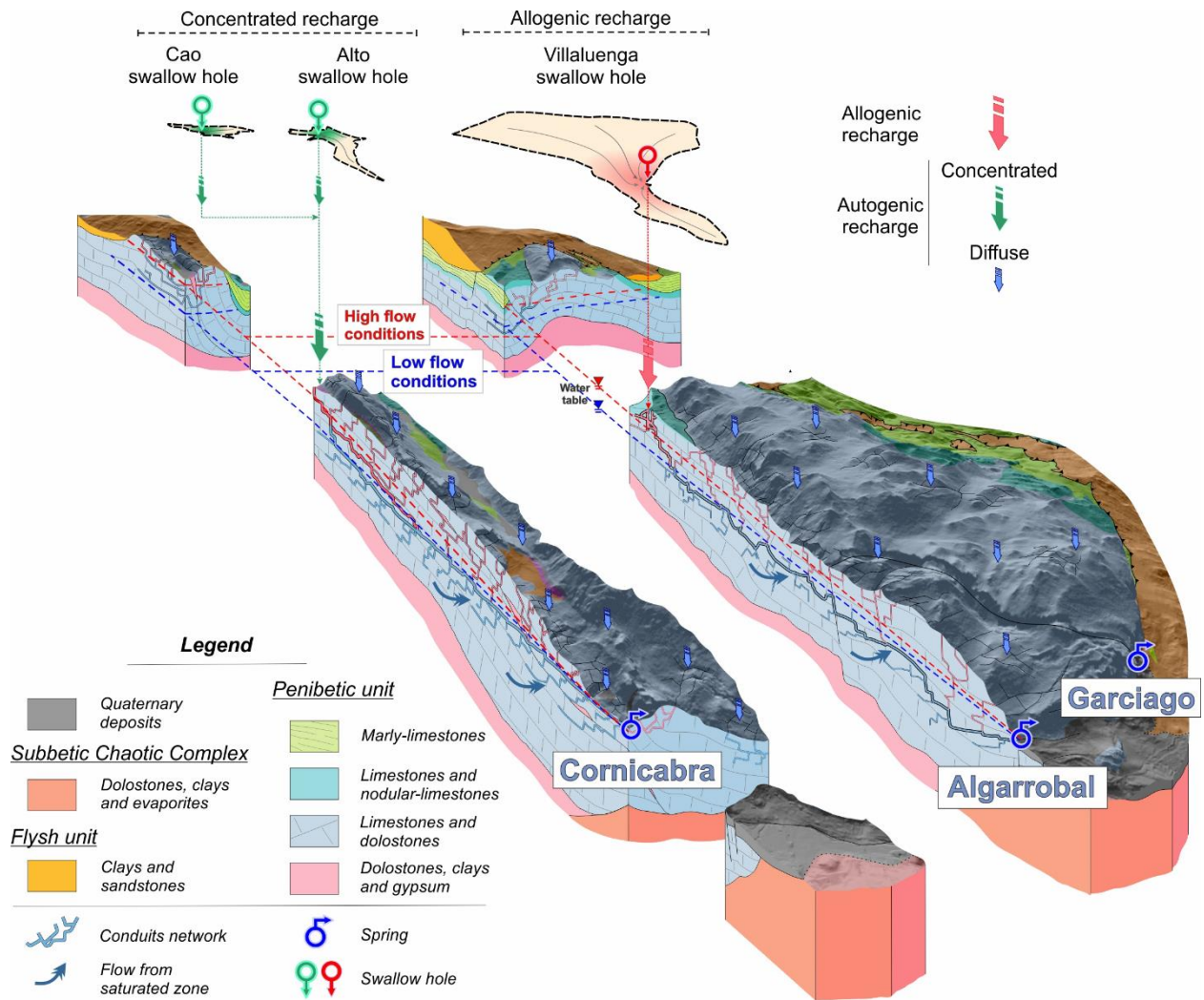
812 Zheng C, Liu J (2013) China’s “Love Canal” moment?, *Science*, 340(6134):810–810, doi
813 10.1126/science.340.6134.810-a

814 Zwahlen F (ed) (2004) *Vulnerability and risk mapping for the protection of carbonate (karst) aquifers. Final report of*
815 *COST Action 620. European Commission, Directorate-General XII Science, Research and Development,*
816 *Brussels.*

817



819
 820 **Fig. 1** Location, geological map and SE-NW oriented hydrogeological cross-section of Ubrique aquifer. Additionally,
 821 confirmed karst connections from the tracer test performed in 2018 are displayed

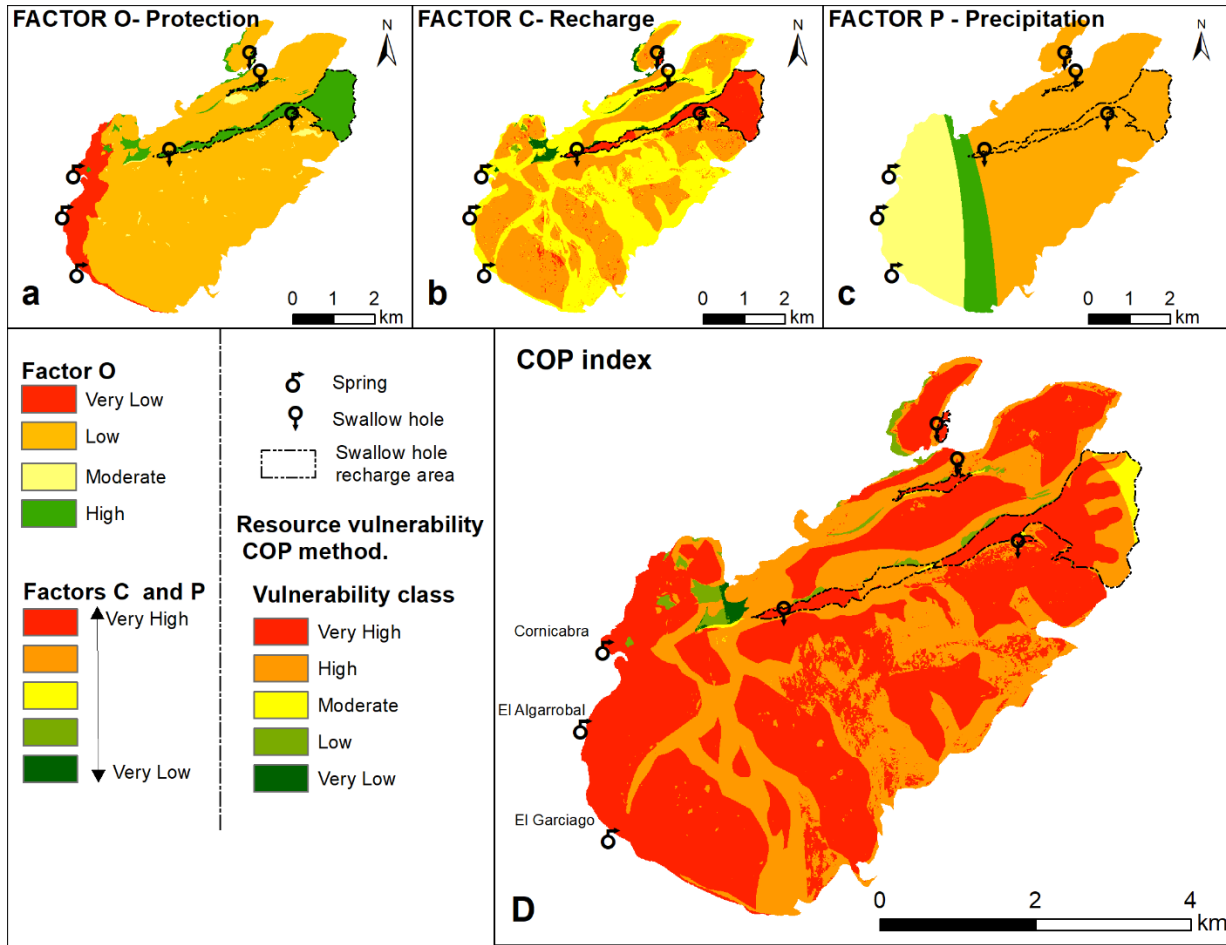


822

823 **Fig. 2.** Hydrogeological conceptual model showing recharge modalities (allogenic *versus* autogenic infiltration),

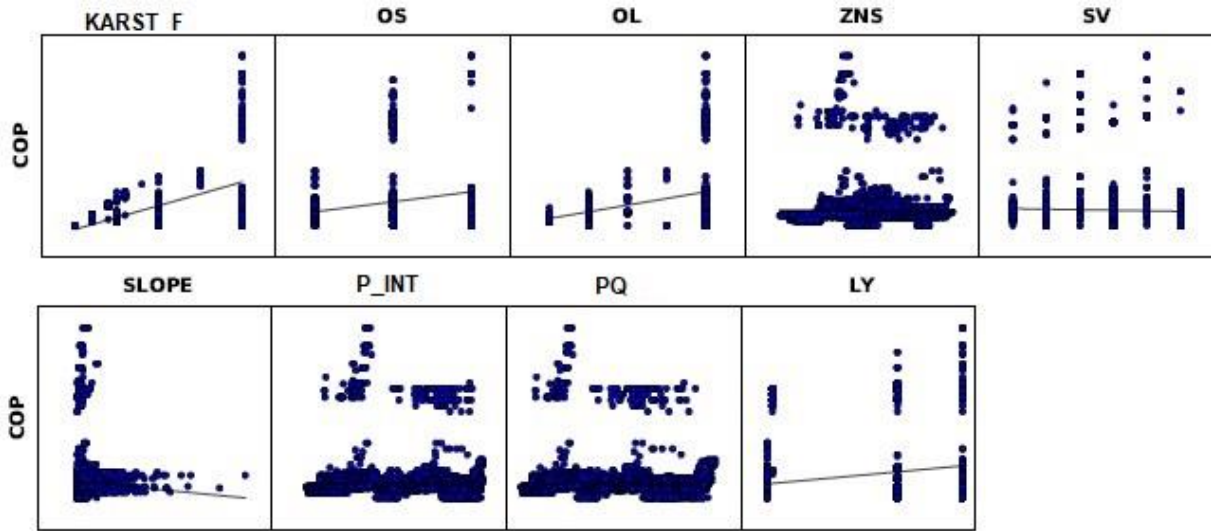
824 sinking points, karst springs, and traced karst flow paths in selected cross-sections (NE-SW oriented) of the Ubrique

825 aquifer



826

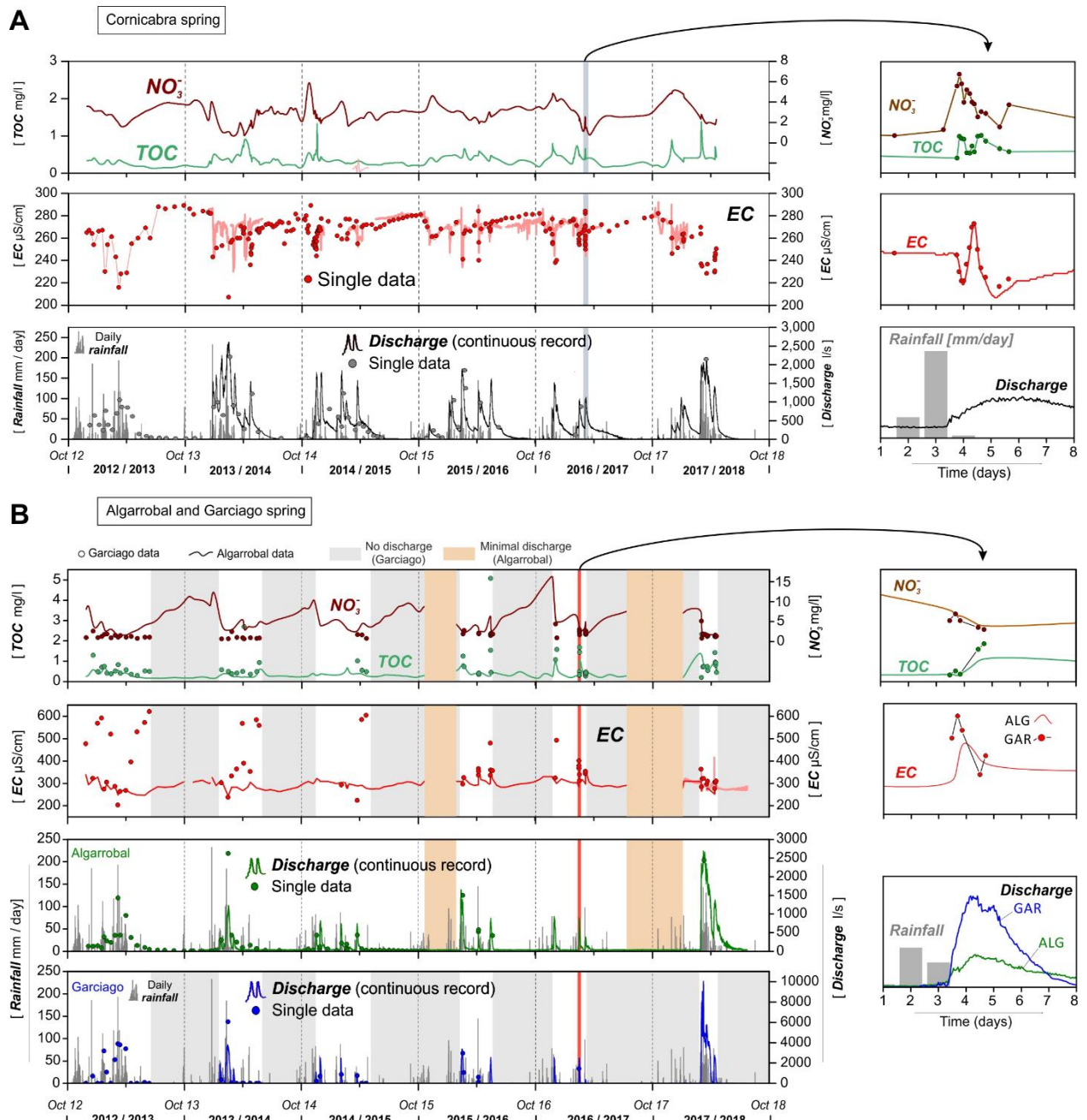
827 **Fig. 3** Maps of resource vulnerability to contamination in the Ubrique aquifer. **a:** factor O, protective capacity of the
 828 overlying layers; **b:** factor C, concentration flow; **c:** factor P, precipitation condition; **d:** COP method, resource
 829 vulnerability classes. Green colours mean favorable conditions (lower degree of vulnerability) and red colours mean
 830 unfavorable conditions (higher degree of vulnerability) for the protection of the groundwater



831

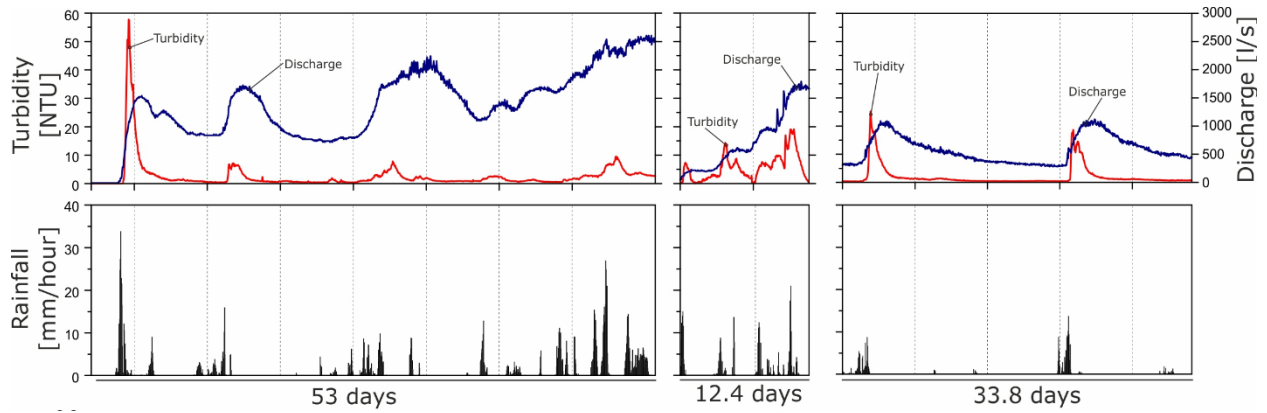
832 **Fig. 4.** Scatterplots for each explanatory variable and the dependent variable. Stronger relationships are depicted as

833 black lines and the slope indicates if the statistical correlation is direct or reverse

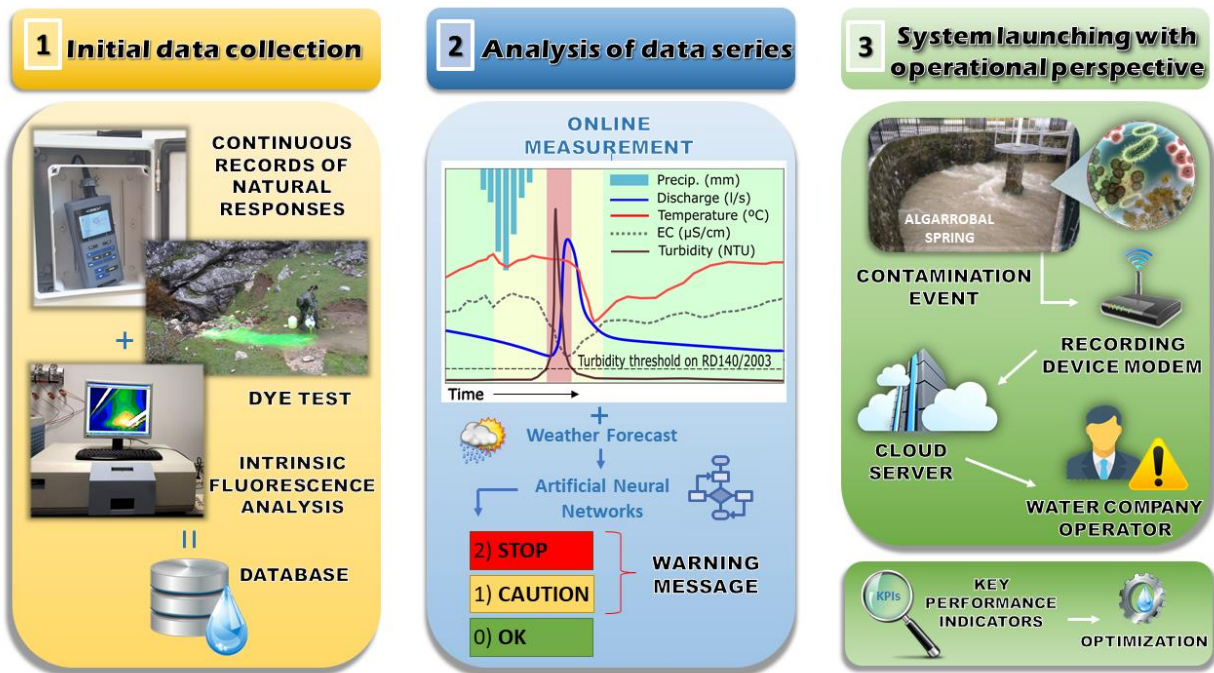


834

835 **Fig. 5** Seasonal (main panels) and single event-based (individual right panels) time evolutions of electrical
 836 conductivity (EC), TOC, and NO_3^- concentrations measured in (a) Cornicabra and (b) Algarrobal and Garciago springs



837
 838 **Fig. 6.** Time series of discharge and turbidity in Algarrobal spring after several rainfall episodes during an
 839 approximately 2-month time window



840
 841 **Fig. 7.** Set-up and implementation steps of the early warning system (EWS) that will be developed in the karst springs
 842 draining Ubrique aquifer (adapted from Grimmeisen et al. 2018)

843

844